AIDIC *Conference Series*, Vol. 10, 2011
Editor Sauro Pierucci
DOI: 10.3303/ACOS1110031

ISBN 978-88-95608-58-7 ISSN 2036-5969

MODELING OF HYDROXYAPATITE PRECIPITATION IN A ROTATING DISK REACTOR

Mariapaola Parisi *, Marco Stoller, Angelo Chianese

University of Rome "La Sapienza", Dept. of Chemical Engineering, Via Eudossiana 18, 00184 Rome, Italy.
* Corresponding author email: mariapaola.parisi@uniroma1.it

In this work the use of a Rotating Disk Reactor for the precipitation of hydroxyapatite is investigated. The adopted device is able to produce nanoparticles in a continuous mode whit relatively low energy consumptions. The required conditions of micromixing can be established in correspondence of the reagents feeding point. The experimental work was mainly devoted to investigate the effect of the reagents feed location over the rotating disk surface. This operating parameter has a great influence on the particle size distribution of the produced HAP and only the optimized position allows the production of particles smaller than 100 nanometers.
The obtained experimental results were interpreted on the light of a hydrodynamic simulation model. The model provided the map of the specific dispersed energy and the flow regimes in the liquid films, thus allowing the identification of the disk zones where micromixing may occur.

1. INTRODUCTION

Hydroxyapatite (HAP) and β-tricalcium phosphate (β-TCP) ceramics have been widely used as bone graft in spine and orthopedic surgery and dentistry. These ceramics exhibited highly biocompatible properties and osteo-conductivity, as demonstrated by several authors. Balasundaram et. al (2006) showed that decreasing the particles size into the nanometer range may promote osteoblast adhesion. HAP is usually produced by a reaction-precipitation process performed by means of a stirring vessel provided by a turbine impeller. This latter apparatus leads to the production of HAP particles several hundreds of nanometers in size.
The main aim of this study is to suggest the use of a Rotating Disk Reactor (RDR) to make the synthesis and precipitation of HAP as a unique apparatus to produce nanoparticles of HAP at industrial level. In fact this intensification process apparatus, as reported by Cafiero et al. (2002) may provide micromixing of the reagents solution over the disk surface at reasonable values of specific dispersed energy. In a previous work, Stoller et al. (2009) pointed out the importance to determine optimal feed location of the reagents on the rotating disk surface in order to achieve the best results. Therefore, the first step in this work was to determine the optimal feed location of the reagents to produce HAP nanoparticles smaller than 100 nm.
Moreover, the obtained results were justified by a simplified simulation model, developed to evaluate the map of the specific dispersed energy over the disk, which is related on the degree of intensification of mixing process between the reagents.

2. EXPERIMENTAL

2.1 The Experimental setup and procedures

The production process of the HAP nanoparticles consisted of the reaction between two aqueous solutions of calcium chloride and ammonia orthophosphate at 50 °C and the subsequent precipitation of the produced HAP. The adopted apparatus is equipped with a disk of 300 mm of diameter rotating at 1500 rpm. The two reagent solutions were separately fed at the same distance from the centre of the disk, as shown in Fig. 1.

Please cite this article as: Parisi M., Stoller M. and Chianese A., (2011), Modeling of hydroxyapatite precipitation in a rotating disk reactor, AIDIC Conference Series, 10, 275-284 DOI: 10.3303/ACOS1110031

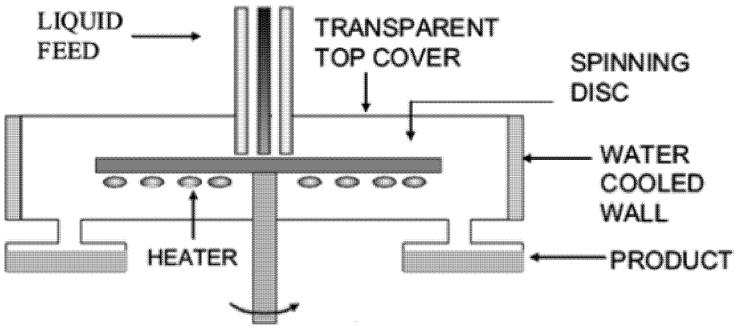

Figure 1: Scheme of the adopted rotating disk reactor.

The feed flow rate of both the reagent solutions was equal to 100 ml/min. A pH value of the overall solution greater than 10 was provided by the injection at the centre of the disk of an aqueous solution of ammonium hydroxide at a flow rate of 80 ml/min: the two reagents are, thus injected on a liquid film constituted by this solution. The ratio between the two reagents were strictly maintained at the stechiometric value equal to 1.67. In order to achieve a high degree of purity for the HAP produced material, the obtained particles were carefully washed with water.
The purity of the produced HAP was evaluated by an IR analysis, measured by the IR instrument model PW1830 supplied by Philips. The particle size distribution was measured by the dynamic light scattering technique: the adopter instrument was the model PLUS 90 supplied by Brookhaven.

2.2 The Experimental results

In order to determine the optimal injection point of the reagents, 3 experimental runs were carried out on the RDR by changing the distance of both reagent injection points, where all the other operating conditions were maintained at the same values, as reported in the former paragraph.
The adopted injection radius, r_{in}, and the obtained mean particle diameters, d, are reported in Table 1.

Table 1: Experimental results for the RDR runs

run ID	r_{in}	d
	mm	nm
1	20	80
2	30	58
3	50	171

The smallest particles are obtained when r_{in} is equal to 30 mm, that is, quite close to the centre of the disc. This optimal position is the same previously reported by Stoller et al. (2009), by using the same RDR for the production of TiO_2 nanoparticles.
The IR spectra of the HAP particles produced in the 3 runs were quite similar. In Fig. 2 the obtained results (full line) are compared with the spectrum of the pure commercial product (dotted line). The good correspondence between the peaks of the two spectra is pretty evident, thus the purity of the produced HAP is satisfactory.

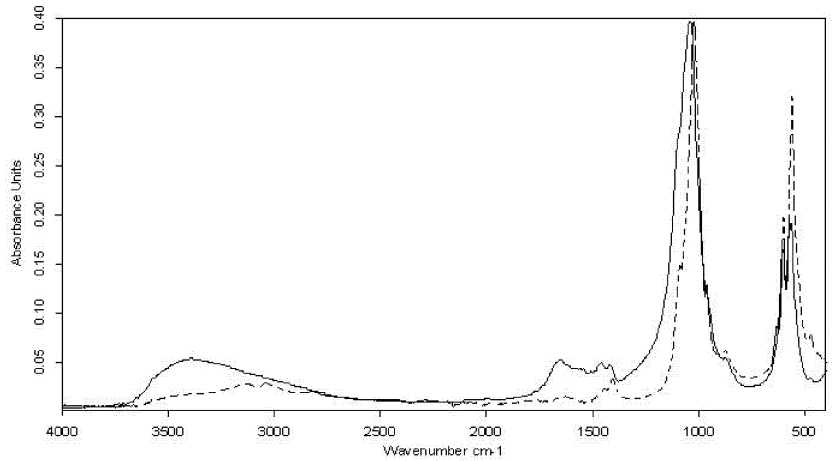

Figure 2: IR analysis of the produced HAP (full line) compared with the one of the pure commercial product (dotted line).

3. THE RDR'S HYDRODYNAMIC MODEL

3.1 The hydrodynamic model

The liquid flow over the surface of a rotating disk can be described by the Navier-Stokes equations for incompressible fluids of constant density in a cylindrical co-ordinate system, r, θ and z (Bird et al., 1960):

$$\rho \cdot \frac{Dv_r}{Dt} - \rho \frac{v_\theta^2}{r} = \mu \cdot \left(\nabla^2 v_r - \frac{v_r}{r^2} - \frac{2}{r^2} \frac{\partial v_\theta}{\partial \theta} \right) - \frac{\partial P}{\partial r} + \rho \cdot g_r \tag{1}$$

$$\rho \cdot \frac{Dv_\theta}{Dt} - \rho \frac{v_\theta \cdot v_r}{r} = \mu \cdot \left(\nabla^2 v_\theta - \frac{v_\theta}{r^2} - \frac{2}{r^2} \frac{\partial v_r}{\partial \theta} \right) - \frac{1}{r} \frac{\partial P}{\partial \theta} + \rho \cdot g_\theta \tag{2}$$

$$\rho \cdot \frac{Dv_z}{Dt} = \mu \cdot \nabla^2 v_z - \frac{\partial P}{\partial z} + \rho \cdot g_z \tag{3}$$

where v_r, v_θ, v_z: are the velocity components along the tree co-ordinates r, θ and z, g_r, g_θ and g_z the gravity acceleration components, P the pressure, μ the viscosity and ρ the density.
The fluid flow is completely described by the system of equations (1)-(3), together with the continuity equation, given by:

$$\frac{1}{r} \cdot \frac{\partial (r \cdot v_r)}{\partial r} + \frac{1}{r} \cdot \frac{\partial v_\theta}{\partial \theta} + \frac{\partial v_z}{\partial z} = 0 \tag{4}$$

The analytical formulation of Navier-Stokes equations can be substantially simplified by the following assumptions (Moore, 1996):

1. the liquid flow is at steady state conditions;
2. the influence of the gravity force is negligible when compared to the effect of the centrifugal force;
3. Coriolis forces are negligible;
4. the effects of the surface tension and shear stress on the liquid free surface are negligible;
5. there is symmetry around the θ axis;

6. the pressure is uniform;
7. the flow regime is laminar;
8. due to the small thickness of the film, the component of the velocity along the z axis is negligible when compared to the components along r and θ. For the same reason $\frac{\partial}{\partial z} >> \frac{\partial}{\partial r}$.

Under the above mentioned hypotheses:

$$-\frac{v_\theta^2}{r} = \nu \cdot \frac{\partial^2 v_r}{\partial z^2} \tag{5}$$

moreover the velocity components along the θ co-ordinate of the liquid and the disk are the same, thus:

$$v_\theta = \varpi r \tag{6}$$

and, combining eqs. (5) and (6):

$$-\varpi^2 r = \nu \cdot \frac{\partial^2 v_r}{\partial z^2} \tag{7}$$

The integration of eq. (7) with the boundary conditions:

$$v_r = 0 \qquad \text{for } z = 0 \tag{8}$$

$$\frac{\partial v_r}{\partial z} = 0 \qquad \text{for } z = \delta \tag{9}$$

where δ is the film thickness, lead to the following expressions for the velocity radial component profile along the z axis, v_r:

$$v_r = \frac{\varpi^2 r}{\nu} \cdot \left(\delta z - \frac{z^2}{2} \right) \tag{10}$$

and, by integrating eq. (10), the mean value of v_r can be calculated:

$$\overline{v}_r = \frac{1}{\delta} \cdot \int_0^\delta v_r dz = \frac{\varpi^2 \cdot r \cdot \delta^2}{3 \cdot \nu} \tag{11}$$

Due to the steady state hypothesis, the layer thickness and the mean radial velocity are connected by the following relation:

$$Q = \overline{v}_r \cdot 2\pi r \cdot \delta \tag{12}$$

where Q is the liquid flow rate. From the eqs. (11) and (12), it follows:

$$\delta = \left(\frac{3}{2\pi} \cdot \frac{\nu \cdot Q}{\varpi^2 \cdot r^2} \right)^{1/3} \tag{13}$$

The liquid residence time and the specific disperse power in a volume of the layer delimited by two generic radial co-ordinates, r_a and r_b, can be computed by the following equations (Cafiero et al.):

$$\tau_{a,b} = \left(\frac{81 \cdot \pi^2 \cdot \nu}{16 \cdot \varpi^2 \cdot Q^2} \right)^{1/3} \cdot \left(r_b^{4/3} - r_a^{4/3} \right) \tag{14}$$

$$\varepsilon_{a,b} = \frac{1}{2 \cdot \tau_{a,b}} \cdot \left[\left(r^2 \cdot \omega^2 - \overline{v}_r^2 \right)_{r=r_b} - \left(r^2 \cdot \omega^2 - \overline{v}_r^2 \right)_{r=r_a} \right] \tag{15}$$

The specific dispersed power determines the micromixing scale lenght:

$$\lambda = \left(\frac{\nu^3}{\varepsilon} \right)^{1/4} \tag{16}$$

and, according to Baldyga and Bourne (1984) the micromixing time may be estimated, on first approximation, as:

$$t_{mix} = 12 \cdot \left(\frac{\nu}{\varepsilon} \right)^{1/2} \tag{17}$$

According to Brauer (1958), for any radial co-ordinate r, the liquid layer surface condition can be determined on the basis of Reynold number:

$$Re = \frac{Q}{2 \cdot \pi \cdot r \cdot \nu} \tag{18}$$

the flow conditions are:

- smooth laminar for Re<4
- lightly waved laminar for 4<Re<10
- waved laminar for 10<Re<20
- turbulent for Re>20.

3.2 Effect of the hydrodynamic conditions on the PSD

It is well known that, in a precipitation process, a fast micromixing leads to a uniform size of the produced particles (Cafiero et al.2002): since the mixing time decreases with the increasing of the specific power, ε, the injection of the two reagents on the ammonium hydroxide solution film should be accomplished where the maximum value of ε is reached. In Fig. 3 the specific dispersed power obtained after the reagents injection, calculated by means of eq. (15) for the adopted operating conditions, is plotted in function of the injection radius.

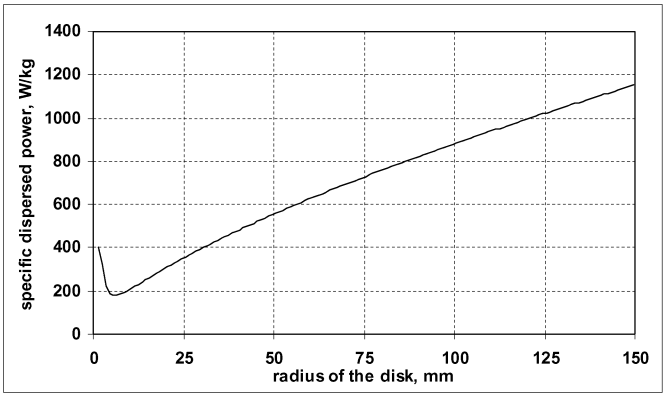

Figure 3: specific dispersed power vs disk radius

From Fig. 3 it appears evident that the injection of the reagents should be accomplished as close to the disk border as possible in order to maximize the dispersed power.
A second aspect that should be considered concerns the residence time on the disk. It is well known that, in a precipitation process, immediately after the nucleation there is some residual supersaturation and nanoparticles tend to aggregate: during this process it is important to avoid the formation of crystalline bridges among the particles by means of high velocity and turbulence. For these reason it should be advisable to maximize the residence time on the disk, where the mixing is efficient, in order to consume the residual supersaturation before the suspension reaches the collecting basin, where there is no mixing device. It is quite evident that, in order to maximise their residence time on the disk, the reagents should be injected in the inner part of the disk. In Fig. 4 the residence time of the reagents on the disk is plotted in function of the injection radius:

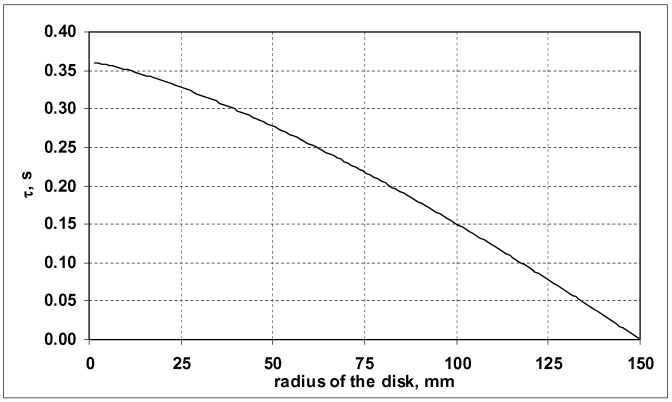

Figure 4: Residence timer vs disk radius

As expected, the residence time decreases as the injection radial position increases: nevertheless the curve is quite smooth for radial position close to the central part of the disk and get sharper close to the border, thus the residence time do not change very much for the injection radiuses adopted for the experimental runs.
Another aspect that may have an influence on the precipitation process is the liquid layer surface condition of the ammonium hydroxide solution in correspondence to the injection point: it is plausible that the presence of waves on the film surface may improve the mixing. In Fig. 5 the profile of the Reynolds number of the ammonia hydroxide solution film, calculated in the adopted operating conditions, is plotted.

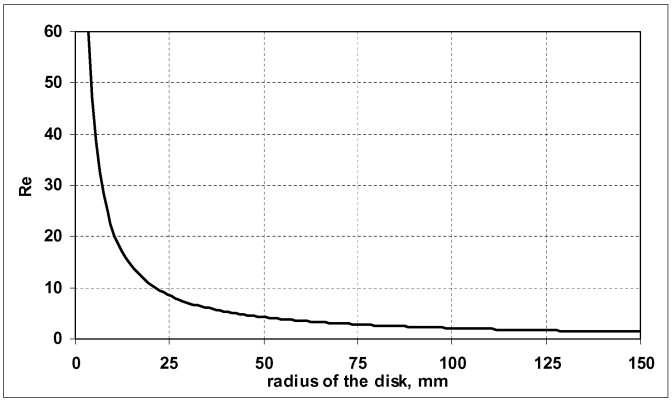

Figure 5: Reynolds number vs disk radius

In the investigated range of injection radiuses, Re varies from 10.6 to 4.2, thus, according to Brauer criterion (1958), the regimes is laminar and the surface is waved with the waved amplitude decreasing as the radius increases. The above considerations may be helpful to interpret the experimental results.

3.3 Comparison between experimental and simulation results

For each run, the following parameters were determined by means of the developed model:

- the layer thickness of the ammonium hydroxide solution in the point of injection of the reagents, δ_{in};
- the Reynolds number of the ammonium hydroxide solution in the point of injection of the reagents, Re_{in};
- the specific power in the point of injection of the reagents, ε_{in};
- the residence time on the disk from the point of injection of the reagents, τ;
- the mixing time, t_{mix};
- the average radial velocity in the point of injection of the reagents, $\overline{v}_{in}$;
- the micromixing length expressed by eq. (11), λ.

The obtained results are reported in Tab. 1.

Table 1:Hydrodynamic parameters for the RDR runs

run ID	δ_{in}	Re_{in}	ε_{in}	τ	t_{mix}	$\overline{v}_{in}$	λ
	μm	#	W/kg	s	ms	m/s	μm
1	39	10.6	296	0.338	0.20	0.62	7.62
2	30	7.1	390	0.321	0.18	0.54	7.12
3	19	4.2	559	0.278	0.15	0.45	6.50

We may observe that the mixing time for every configuration is smaller than 1 ms and the Kolmogorov micromixing scale is lower than 10 μm. These conditions are characteristics of the attainment of micromixing between the reagents, which assure a mixing time smaller than the nucleation induction time, expected equal or greater than 1 ms. The average size of the particles in the three different cases is determined by both the number of nanoparticles locally generated and their aggregation grade due to the particles collisions under a residual supersaturation. If we assume that in any case we have the same number of generated nanoparticles, the remarkable increase of the particles size for an injection at 5 cm from the centre is mainly due to a higher

aggregation rate. This fact is justified by the lower Reynolds number and lower radial velocity which enhance the probability of particles collisions. Recently Bhatelia et al (2009) made a 3D simulation of a liquid layer over an RDR 3.5 cm in diameter and showed that there is a waveless laminar regime in the initial section followed by asymmetric wave formation, turbulent region and a second laminar-wave region near the outer perimeter. A similar approach was recently attempted at the Industrial Crystallization Laboratory of the University of Rome and similar results were obtained, as reported elsewhere (de Caprariis, 2011). The injections zone corresponding to the first two cases, examined in this work, should be, thus, characterized by the presence of asymmetric waves which leads to a further reduction of the particles collisions.

4. CONCLUSIONS

The continuous production of nanoparticles of HAP, that is smaller than 100 nm in size, is possible by using a RDR and by optimizing the location of the feed points of the reagents. In fact, in this work HAP nanoparticles down to 58 nm in size were produced. A simplified model developed to predict the hydrodynamics of the liquid over the disc and the specific energy dispersion map was successfully used for the interpretation of the experimental results. However, for this purpose a more rigorous model, based on the CFD technique, could be useful. Finally, it has to be noticed that the applied reaction conditions, together with the subsequent washing of the produced nanoparticles, allowed the production of HAP material of high purity.

5. LIST OF SYMBOLS

d	particles diameter, nm
g	gravity acceleration, m/s^2
P	pressure, Pa
Q	volumetric flow rate, m^3/s
r	radial co-ordinate, m or mm
Re	Reynolds number, dim.less
t	time co-ordinate, s
t_{mix}	micromixing time, s or ms
v	velocity, m/s
z	axial co-ordinates, m or mm

5.1 Greek letters

δ	liquid film thickness, m or μm
ε	specific dispersed power, W/kg
θ	angular co-ordinate, rad
λ	Kolmogorov micromixing scale length, m or μm
μ	dynamic viscosity, Pa·s
ν	kinematic viscosity, m^2/s
ρ	liquid density, kg/m^3
τ	residence time, s
ω	angular velocity, rad/s

5.2 Under scripts

in	radial position corresponding to the injection point
a	generic radial position
b	generic radial position

r Component along the r co-oridante
θ Component along the θ co-ordinate
z Component along the z co-oridante

6. REFERENCES

Balasundaram G., Sato M., Webster T.J., 2006, Using hydroxyapatite nanoparticles and decreased crystallinity to promote osteoblast adhesion similar to functionalizing with RGD, Biomaterials 27, 2798–2805.

Baldyga, J. and Bourne, J.R., 1984, A fluid mechanical approach to turbulent mixing and chemical reaction: Micromixing in the light of turbulence theory, Chem. Eng. Commun., 28, 243-258.

Bhatelia, T.J., Utikar, R.P., Pareek, V.K. and Tade, O.M., 2009, Characterizing liquid film thickness in spinning disc reactors, Proceedings of the Seventh International Conference on CFD in the Minerals and Process Industries, CSIRO, Melbourne, Australia, 9-11 December 2009.

Bird R.B., Stewart W.E., Lightfoot E.N., 1960, Transport Phenomena, Wiley & Sons, New York.

Brauer H., 1958, Stoffaustausch beim Rieselfilm, Chem. Ing. Tech, 30 (2), 75 -84.

Cafiero M.L., Baffi G., Chianese A., Jachuck R., 2002, Process Intensification: Precipitation of Barium Sulphate Using a Rotating Disk Reactor (RDR), Industrial Engineering Chemistry Research 41, 5240-46.

de Caprariis B., Verdone N., Parisi M., Chianese A., 2011, CFD Modeling of a Rotating Disk Reactor, Proc. of the 18th International Symposium on Industrial Crystallization, Zurich, 13-16 September 2011.

Moore, S. R., 1996, Mass Transfer to Thin Liquid Films on Rotating Surfaces, with and without Chemical Reaction, Ph.D. Dissertation, University of Newcastle upon Tyne, Newcastle upon Tyne, U.K.

Stoller M., Miranda L., Chianese A., 2009, Optimal feed location in a rotating disk reactor for the production of TiO2 nanoparticles, Chemical Engineering Transactions 17, 993-998.